



HAL
open science

Carbon screen-printed electrodes modified by a polycatechol film for Cu and Pb detection in acidified drinking water

Corinne Parat, Estelle Ricard, Wahid Ben Mefteh, Isabelle Le Hécho

► To cite this version:

Corinne Parat, Estelle Ricard, Wahid Ben Mefteh, Isabelle Le Hécho. Carbon screen-printed electrodes modified by a polycatechol film for Cu and Pb detection in acidified drinking water. *Electrochimica Acta*, 2023, 461, pp.142666. 10.1016/j.electacta.2023.142666 . hal-04142593

HAL Id: hal-04142593

<https://univ-pau.hal.science/hal-04142593>

Submitted on 27 Jun 2023

HAL is a multi-disciplinary open access archive for the deposit and dissemination of scientific research documents, whether they are published or not. The documents may come from teaching and research institutions in France or abroad, or from public or private research centers.

L'archive ouverte pluridisciplinaire **HAL**, est destinée au dépôt et à la diffusion de documents scientifiques de niveau recherche, publiés ou non, émanant des établissements d'enseignement et de recherche français ou étrangers, des laboratoires publics ou privés.

Carbon screen-printed electrodes modified by a polycatechol film for Cu and Pb detection in acidified drinking water

Corinne Parat*, Estelle Ricard, Wahid Ben Mefteh, Isabelle Le Hécho

CNRS / Univ Pau & Pays Adour / E2S UPPA, Institut des sciences analytiques pour l'environnement et les matériaux, UMR5254, 2 avenue Pierre Angot, 64000 Pau, France

*corresponding author: corinne.parat@univ-pau.fr

Abstract

The dissolution of metals such as Cu or Pb in water can be increased by prolonged stagnation of water in internal pipes of drinking water networks, resulting in high concentrations in the consumer's tap water. As they can accumulate in biota and affect living organisms with more or less serious long-term toxic effects, the monitoring of Cu or Pb in tap water and more generally in aquatic environments is therefore an important issue. For this purpose, a new electrochemical sensor based on a screen-printed carbon electrode modified with a polycatechol film was developed for the highly sensitive detection of Cu and Pb in drinking water. The electropolymerisation was first optimised to obtain a homogeneous and reproducible film for the detection of trace metals. The mechanism of the polymerization process was proposed and discussed. Then, the performance of the new sensor was evaluated. The pH and the conductivity were found to be the main parameters influencing the sensitivity of the sensors. Thus, the electrochemical analyses carried out at pH values around neutrality with this device made it possible to determine the free and labile forms of metal in solution, while the total metal contents were determined after acidification of water samples to pH 5 or less. Furthermore, a stable signal was obtained from $470 \mu\text{S cm}^{-1}$, which means that most of freshwater rivers and mineral waters can be directly analysed without any supporting electrolyte addition. After optimisation of the analytical conditions, a

30 sensitivity of the order of $\mu\text{g L}^{-1}$ was reached for a deposition time of 60 s while an
31 electrodeposition time of 300 s gave a sensitivity of ng L^{-1} .

32

33 **Keywords:** Electropolymerisation, *in situ* detection, trace metals, stripping
34 chronopotentiometry

35

36

37 **1. Introduction**

38 The presence of metals such as lead (Pb) and copper (Cu) in water leaving water
39 production facilities is low or undetectable. However, these substances can be found in
40 higher concentrations in the consumer's tap water due to the dissolution of these metals
41 in the water contained in the pipes (internal networks and possibly public connections),
42 valves and fittings of the internal networks of buildings [1]. Concentrations in drinking
43 water vary from 0.005 to 30 mg/L for Cu, mainly due to corrosion in internal Cu pipes,
44 and are generally below 5 $\mu\text{g/L}$ for Pb, although much higher concentrations (above 100
45 $\mu\text{g/L}$) have been measured in the presence of Pb pipes or fittings [2]. While there is still
46 some uncertainty regarding the long-term effects of copper on sensitive populations [3], this is
47 not the case of Pb which is recognized as a chemical of high public health concern.
48 Thus, the quality limit in water intended for human consumption is currently set at 10
49 $\mu\text{g/L}$ for Pb and at 2 mg/L for Cu by Directive 2020/2184 in accordance with the guide
50 value recommended by the World Health Organisation (WHO) [4].

51 According to WHO, exposure must be assessed using an appropriate sampling strategy,
52 taking into account when, where, and how samples are collected, as well as the number
53 of samples to be collected [5]. Monitoring of metals in tap water and more generally in
54 aquatic environments is therefore an important issue as they can accumulate in the biota
55 and affect living organisms with more or less serious long-term toxic effects [6, 7].
56 Among the available analytical techniques, only a few approaches allow the
57 implementation of suitable *in situ* devices in terms of analytical performance,
58 autonomy, miniaturization feasibility, and ease of transport [8]. Due to their high
59 sensitivity, electrochemical techniques, such as anodic stripping voltammetry (ASV)
60 and stripping chronopotentiometry (SCP) using disposable sensors, have proven to be
61 promising approaches for the analysis of metals in freshwater [9-14]. Among one single-

62 use sensors, screen-printed electrodes have been increasingly studied due to their
63 performance and ability to be mass-produced at very low costs [15-18]. In addition,
64 their surface can be easily modified, which has led to different improvements in the
65 final sensor, such as increased selectivity and/or sensitivity. Most screen-printed sensors
66 for sensitive determination of metals were based on a mercury film as a modifier of the
67 working surface [19-21]. Due to the toxicity of mercury, several new types of mercury-
68 free film electrodes have been developed for trace metal detection, such as bismuth-
69 coated carbon electrodes [22-24] or gold-film electrodes [25-28]. Recent achievements
70 show the electrochemical detection of trace metals with electrodes modified with
71 inorganic, organic and biological materials [29-31]. Metal, metal oxide, carbon and
72 silica-based nanomaterials have emerged as the most commonly used nanomaterials for
73 electrochemical detection of trace metals [17, 32, 33]. Organic polymers have also been
74 widely employed in sensor construction [34, 35]. Polyaniline, polypyrrole and poly(3,4-
75 ethylenedioxythiophene) are the main conductive polymers used for biosensors due to
76 their low-cost synthesis, high sensitivity, and excellent stability [36]. Catechol is a
77 simple molecule, capable of establishing a wide range of interactions with organic and
78 inorganic analytes [37, 38]. Depending on the pH, it also showed a tendency to form
79 mono-, di-, or tri-coordinated complexes with metals like Cu, Zn, Ni, Co, Mn, Fe [39-
80 42]. Thus, Koo *et al* demonstrated that a polycatechol film deposited on a glassy carbon
81 electrode allowed the preconcentration of Ce(III) before its detection by differential
82 pulse anodic stripping voltammetry [43].

83 All these works suggest that polycatechol is a good candidate for the development of an
84 electrochemical sensor for *in situ* trace metal detection. The present study focused on
85 the original development of an electrochemical sensor for Cu and Pb monitoring in
86 drinking water. Our objective was to modify the working surface of a screen-printed
87 electrode by a polycatechol film in order to form a time-stable, low-cost, robust and
88 sensitive electrochemical platform for a direct metal detection in a freshwater sample.
89 After optimizing the electrodeposition of the polycatechol film on a carbon-based
90 screen-printed electrode (SPCE), the performance of the modified sensor for Cu and Pb
91 detection was investigated and then tested in a mineral water sample.

92

93 **2. Experimental**

94 **2.1 Chemicals and reagents**

95 The polystyrene support for the screen printing was obtained from Sericol. The
96 commercial ink (electrodag PF-407A) was purchased from Acheson Colloids. Acetic
97 acid (CH_3COOH , Trace select), sodium acetate trihydrate (CH_3COONa , Trace select)
98 were obtained from Fluka. Nitric acid (69-70%, Baker Instra-Analysed for trace metal
99 analysis) and sodium hydroxide (Baker Analysed) were obtained from J.T. Baker.
100 Mesitylen, disodium hydrogen phosphate dihydrate ($\text{Na}_2\text{HPO}_4 \cdot \text{H}_2\text{O}$), sodium phosphate
101 monobasic (NaH_2PO_4) and 1,2-dihydroxybenzene (catechol) were purchased from
102 Sigma-Aldrich. The stock solutions at 1000 mg L^{-1} of Cu and Pb were obtained from
103 Merck. Ultrapure water (resistivity of $18 \text{ M}\Omega \text{ cm}$) was used for dilutions. Acetate buffer
104 solution (0.1 mol L^{-1} , pH 4.6) was prepared by mixing appropriate amounts of
105 CH_3COOH and CH_3COONa . Phosphate buffer (0.1 mol L^{-1} , pH 7.5) was prepared by
106 mixing appropriate amounts of Na_2HPO_4 and NaH_2PO_4 . Chemical composition of the
107 mineral water was: calcium 68 mg L^{-1} , potassium 11 mg L^{-1} , magnesium 2 mg L^{-1} ,
108 sodium 21 mg L^{-1} , bicarbonates 219 mg L^{-1} , chlorides 28 mg L^{-1} , sulphates 39 mg L^{-1} ,
109 nitrates 1 mg L^{-1} , pH 7.6, conductivity $476 \mu\text{S cm}^{-1}$ (equivalent to 285 mg L^{-1}).

110

111 **2.2 Instruments**

112 All electrochemical measurements were performed on an Eco Chemie $\mu\text{Autolab III}$
113 connected to a Metrohm 663 VA Stand and a computer using the GPES 4.9 software
114 package (Eco Chemie). Electrochemical measurements were performed by means of a
115 three electrode-system: a screen-printed carbon electrode (SPCE) with an active area of
116 9.6 mm^2 as working electrode, a carbon auxiliary electrode and an Ag/AgCl KCl (3 mol
117 L^{-1}) reference electrode encased in a 0.1 mol L^{-1} KNO_3 jacket. A 3mm diameter glassy
118 carbon electrode (GCE) from Syclope Electronique was also tested as a working
119 electrode.

120

121 **2.3 Preparation of catechol modified screen-printed electrode**

122 The electrodes were manually screen printed on 1 mm-thick polystyrene plates using a
123 commercial carbon-based ink to produce a set of 8 electrodes (Figure S1) [10]. After a
124 drying step (1 hour at room temperature) and a curing step (1 hour in an oven at 60°C),
125 an insulating layer (polystyrene dissolved in an adequate volume of mesitylene) was
126 manually spread over the conductive track, leaving a working disk area of 9.6 mm^2 and
127 an electrical contact.

128 The electrodeposition of catechol (1,2-Dihydroxybenzene) on the SPCE working
129 surface was carried out in three steps. The following conditions correspond to the
130 optimised conditions. The first step was the electrodeposition of catechol (10 mmol L^{-1})
131 on the working surface by cyclic voltammetry (CV) between -0.8 V and $+0.8 \text{ V}$ versus
132 Ag/AgCl at scan rate of 200 mV s^{-1} in phosphate buffer (pH 7.2). The modified
133 electrode was characterized by CV at 200 mV s^{-1} , using a monomer-free acetate buffer
134 solution (pH 4.8). In a second step, the electrode was rinsed with water, immersed in 0.1
135 mol L^{-1} NaOH and cycled until a stable baseline was obtained. The final step was to air
136 dry for 24 hours. The sensor is stored in the open air when not in use.

137

138 **2.4 Electrochemical measurements**

139 Trace metal measurements were performed at room temperature in a 0.1 mol L^{-1} acetate
140 supporting electrolyte at pH 4.8 by SCP. Like the usual stripping voltammetry
141 techniques, SCP requires two steps: a deposition (accumulation) step in which metal
142 ions are reduced at a constant potential, followed by a stripping (quantification) step
143 involving reoxidation by applying a constant oxidising current. The analytical signal is
144 the time required for reoxidation (transition time τ). A reliable determination of τ is
145 obtained by measuring the area under the peak in the dt/dE versus E plot, where dt/dE is
146 the inverse of the time (t) derivative of the recorded potential (E) [44, 45]. After
147 optimisation, the analytical parameters were as follows: an electrodeposition step of 60
148 s at -1.2 V with stirring, followed by an equilibration time of 10 s at -1.2 V without
149 stirring and a stripping step by applying a stripping current (I_s) of $10 \text{ }\mu\text{A}$ without
150 stirring.

151

152 **2.5 Analytical performance**

153 Analytical performance (sensitivity, limit of detection and limit of quantification) of the
154 modified SPCE was investigated using SCP, an analytical technique that allows the
155 detection of trace metals at low concentrations (in the $\mu\text{g L}^{-1}$ range) by applying the
156 electrochemical parameters described above. Analyses were performed without purging
157 at room temperature in a 0.1 mol L^{-1} acetate supporting electrolyte at pH 4.6, doped in
158 Cu or Pb. Validation of the sensor was performed by SCP in a mineral water acidified at
159 pH 4.6 with acetic acid, and doped in Cu at $40 \text{ }\mu\text{g L}^{-1}$ in order to determine the total Cu
160 concentration.

161

162 **2.6 Statistical approach**

163 The reliability of the sensor manufacture was based on the reproducibility, which was
164 investigated by first comparing 8 modified SPEs from the same screen-printing plate
165 (intra-plate reproducibility) and then by comparing 8 modified SPCEs from 8 different
166 screen-printing plates (inter-plate reproducibility) (Figure S1). For each sensor, the
167 mean Cu signal and its standard deviation, based on three replicates, were determined
168 for a Cu concentration of 20 $\mu\text{g L}^{-1}$ in a 0.1 mol L^{-1} acetate buffer.

169 The linearity and the sensitivity were obtained from the calibration plot based on 3
170 replicate analyses for each concentration. The linear regression analysis was performed
171 by using the least squares method with the Excel analysis toolpak. This method was also
172 used to calculate the slope and the intercept as well as their respective standard
173 deviation.

174

175 The limit of detection (LOD) has been statistically determined from the calibration plot
176 according to Eq. (1)

$$177 \quad LOD = kS_b/m \quad (1)$$

178 where $k = 3$, S_b is the intercept standard deviation of the regression line and m is the
179 slope of the linear calibration plot [46]. The limit of quantification (LOQ) was
180 calculated with the same equation as for the detection limit; however, the k-value was
181 taken to be 10.

182

183 **2.7 Speciation model**

184 The geochemical modelling program *Visual Minteq*, ver. 3.0 (using the standard
185 databases) [47] was used to predict metal speciation in mineral water. The following
186 inputs were provided: pH, temperature (25°C), and total concentrations for Ca, Na, K,
187 Mg, carbonates, nitrates, sulfates, chlorides, Cu and Pb.

188

189 **3. Results and discussion**

190 **3.1 Electrochemical behaviour of catechol on SPCE**

191 The functionalization of the transducer is an important step in the development of an
192 electrochemical sensor, as it will determine the performance of the electrodes in terms

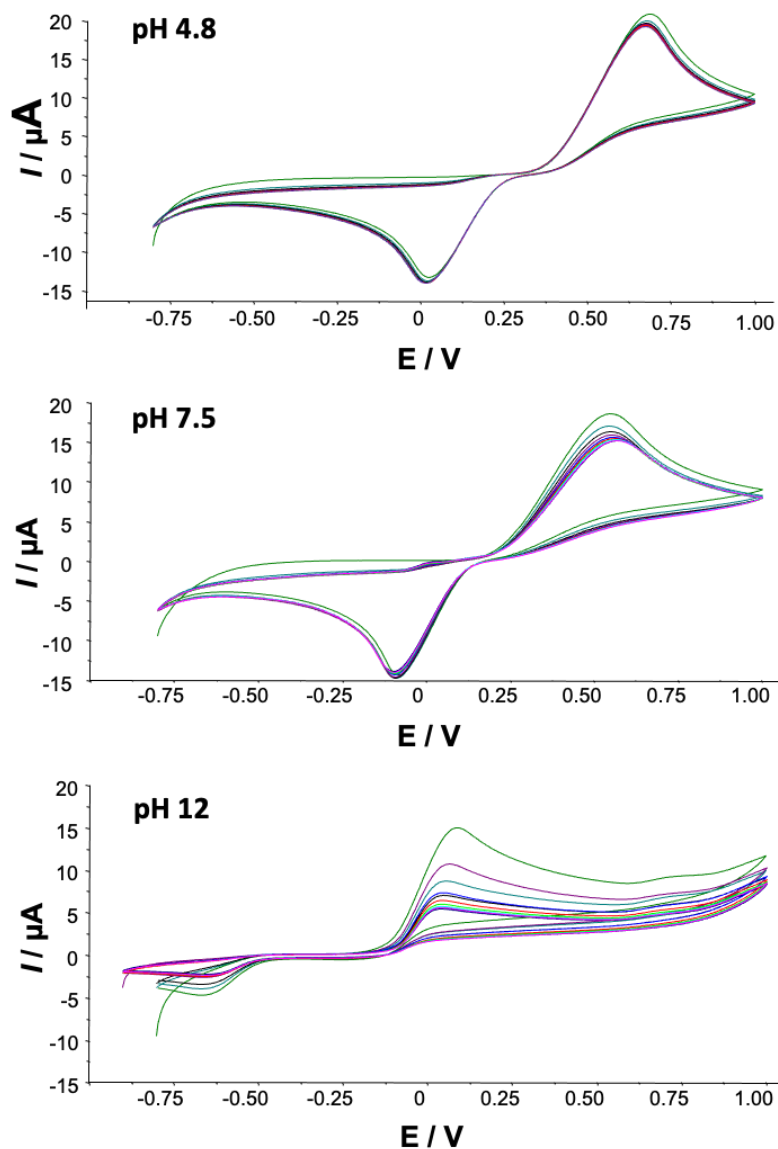
193 of sensitivity and stability over time. Our objective was first to optimise the
194 electropolymerisation of catechol to obtain a stable and reproducible polycatechol film.
195 Firstly, two types of electrodes were tested, SPCE and GCE. CV electropolymerisation
196 of catechol showed that consecutive scans do not lead to a change in the anodic peak,
197 suggesting that the polymer does not deposit on the GCE surface (Figure S2).
198 Comparison of the electrode surfaces suggested that the rough surface of SPCE was
199 more favourable for electropolymerisation than the smooth surface of GCE (Figure S3).
200

201 3.1.1 Effect of pH during electropolymerisation

202 As expected, CV performed in a solution of catechol at different pH values shows that
203 redox processes are pH dependant (Figure 1). Whatever the pH, the first potential scan
204 shows an anodic peak related to the oxidation of catechol to o-benzoquinone and a
205 corresponding cathodic peak related to the reduction of o-benzoquinone to catechol.
206 This redox process involves the transfer of two electrons and two protons [48, 49]. The
207 following scans show a different behaviour depending on the pH. At acidic pH, the
208 subsequent scans lead to a slight decrease of the anodic peak (5%) coupled with the
209 appearance of a second oxidation peak at 0.21V, whose intensity increases with the
210 cycles, suggesting the formation of a redox-active polymer film on the electrode surface
211 [50]. This behaviour appears much more pronounced at neutral pH with the appearance
212 of a second oxidation peak at 0.01V and a decrease in the catechol oxidation peak by
213 22% after 10 scans. The highest pH leads to a marked decrease in peak height (64%)
214 with the appearance of a second oxidation peak at 0.72V suggesting a rapid
215 dimerisation process in solution, leading to the depletion of catechol [48].

216

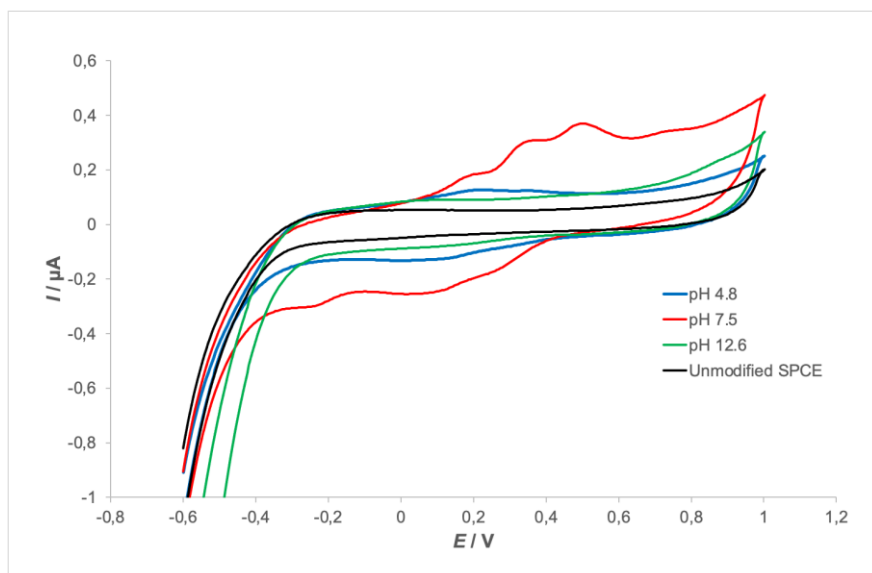
217



218 **Figure 1.** Electropolymerization of 0.5 mmol L^{-1} of catechol at different pH 4.8, 7.5 and 12.6. Cyclic
 219 voltammetry from -0.8 to 1V at 200 mV s^{-1} . First scan is represented in green and last scan in purple.
 220

221
 222 In order to check the deposition of the polycatechol film, CV were performed in acetate
 223 buffer solution without catechol. **Erreur ! Source du renvoi introuvable.** confirms that
 224 the polymerisation pH leads to different mechanisms of electrodeposition. An acidic pH
 225 allows the formation of a slightly electroactive film with only one redox couple. A basic
 226 pH does not lead to any significant modification of the electrode, compared to an
 227 unmodified electrode, which confirms the absence of polymerisation at this pH. On the
 228 contrary, neutral pH seems to be the most favourable for the formation of an
 229 electroactive polymer on the electrode surface with 3 redox couples observed in the
 230 blank solution, immediately after electropolymerisation [50]. These observations are in
 231 agreement with those of Marczewska (2013) who showed that the polymerisation
 232 process works from weakly acidic medium (pH 5.4) to weakly alkaline medium (pH

233 9.2) [51]. Moreover, it is interesting to note that air drying of the modified electrodes
234 leads to a strong decrease in these redox peaks (not shown) suggesting an irreversible
235 oxidation of the polymer by oxygen in the air. For this reason, the modified electrodes
236 were then air-dried for 24 hours before use.
237



238
239 **Figure 2.** Cyclic voltammograms of polymerized SPCE at different pH in a blank solution (acetate buffer,
240 0.1 M, pH 4.8). Scan rate: 200 mV s⁻¹.
241

242 The proposed mechanism to explain the formation of an electroactive film on the
243 electrode is the formation of a polymer *via* the coupling of mesomeric structures of
244 phenoxy radical [52, 53]. Ortho-semiquinones, formed during the reduction steps from
245 orthoquinones, are highly reactive species capable of reacting to form higher oligomers
246 resulting in film deposition. When two of these ortho-semiquinones are sufficiently
247 close, they undergo aryl-aryl coupling and progressive film deposition by
248 polymerisation [54].

249 We can therefore conclude that the polymerisation process is initiated by the production
250 of free radicals following the electrochemical oxidation of catechol to benzoquinone
251 and its subsequent reduction to ortho-semiquinone (Figure S4). Once this radical
252 initiator is formed, it attacks another monomer to initiate a polymer chain. Redox cycles
253 allow the chain to propagate. Termination occurs during air drying, with oxygen acting
254 as a polymerisation inhibitor.

255 The acidity dissociation constants (pK_a) for its hydroxyl groups are both above 7: pK_{a1}
256 = 8.83 and pK_{a2} = 13.07 [55]. Changing the pH of the catechol solution leads to a
257 change in and the dissociated forms and their concentration. Thus, at pH 7.5, the

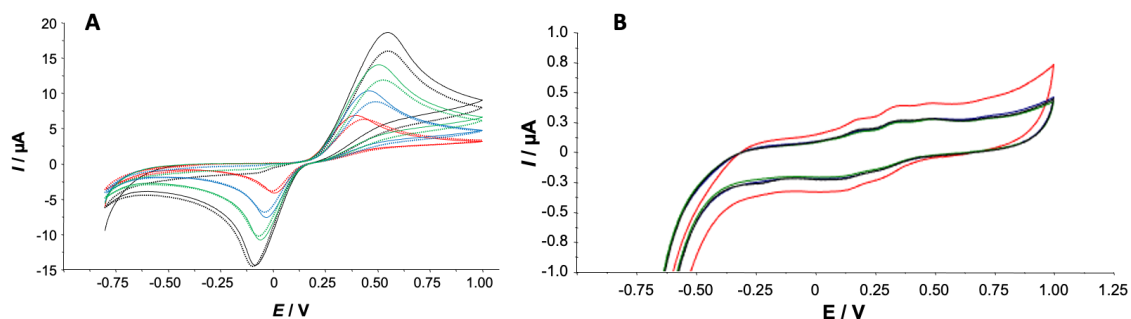
258 monoanion starts to form (between 2 and 4% depending on the pK_a value) whereas at
259 pH 12, the catechol is in anionic form only. At higher pH, Pourghobadi *et al* proposes
260 an alternative mechanism based on anionic or dianionic forms of catechol as
261 nucleophiles that would rapidly add to the electrochemically generated o-benzoquinone,
262 the rate of the dimerisation reaction increasing with pH [56].
263 As our objective was to optimize and control the deposition of the film catechol on the
264 surface of the working electrode, a pH of 7.5 was chosen for catechol
265 electropolymerisation.

266

267 3.1.2 Effect of scan rate during electropolymerisation

268 Figure 3A shows the first and 10th scan obtained during electropolymerisation with
269 different scan rates from 20 (red line) to 200 mV s^{-1} (black line) in a phosphate buffer
270 solution (0.1 M, pH 7.5) containing 0.5 mmol L^{-1} of catechol. Increasing the scan rate
271 induces an increase in peak height (x2.5), and in ΔE_p (from 0.38 to 0.61V). The effect of
272 scan rate on the properties of the polymer film was then studied in an acetate buffer
273 solution at pH 4.6 (Figure 3B). Regardless of the scan rate, the polymerization of
274 catechol leads to a film with 3 redox reactions (3 redox peaks). The lowest scan rate
275 results in the highest capacitive current, while the other 3 scan rates give exactly the
276 same voltammogram (Figure 3B). The slower the potential scan rate, the longer the life
277 time of the semi-quinone radicals and the higher the probability of depositing thicker
278 films with larger oligomers [54]. On the contrary, a high scan rate (200 mV s^{-1}) allows
279 linear polymer growth due to a conductive and/or porous polymer matrix [57].
280 Therefore, a scan rate of 200 mV s^{-1} was chosen for the next experiments.

281



282

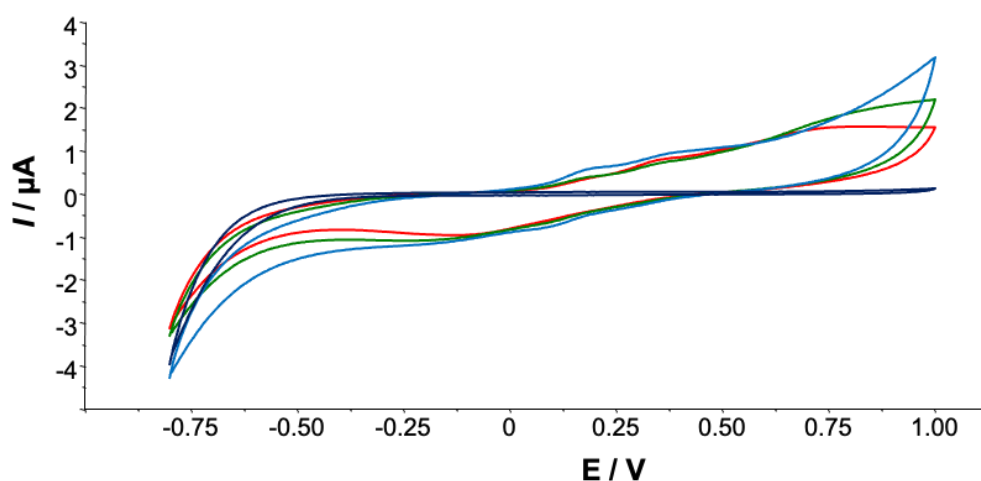
283 **Figure 3.** CV of polymerized SPCE at different scan rates: red line: 20 mV s^{-1} , blue line: 50 mV s^{-1} , green
284 line: 100 mV s^{-1} and black line: 200 mV s^{-1} in a 0.5 mmol L^{-1} catechol solution (pH 7.5). **A** - first scan
285 (solid line) and last scan (dotted line) of catechol film polymerization; **B** - CV in a 0.1 M acetate buffer
286 solution (pH 4.8; scan rate: 200 mV s^{-1}).

287

288 3.1.3 Effect of scan number during electropolymerisation

289 Figure 4 shows the effect of the number of scans on the properties of the polymer film.
290 The polymer films obtained after 10, 20 or 50 scans show similar behaviour.
291 Voltammograms obtained in acetate buffer solution show that the capacitive current
292 does not increase with the number of polymerisation cycles suggesting that the polymer
293 is porous and/or conductive (Figure 4). According to Almeida *et al.*, the mass growth
294 profile of polycatechol is approximately linear during the 50 polymerization cycles due
295 to the continuous oxidation of catechol at the electrode surface [38]. Consequently, an
296 electropolymerisation of catechol based on 50 CV was retained for the following
297 experiments which aim to detect trace metals in freshwater samples.

298



299

300 **Figure 4.** CV of polymerized SPCE from different scan number (black line: unmodified SPCE, red line:
301 10 scans, green line: 20 scans and blue line: 50 scans) in a blank solution (acetate buffer 0.1 M at pH 4.8;
302 scan rate: 200 mV s⁻¹).

303

304 **3.2 Electrochemical detection of Cu and Pb by stripping** 305 **chronopotentiometry**

306 3.2.1 Optimization of the stripping current

307 By varying the applied stripping current, the stripping time regime can be varied from
308 semi-infinite linear diffusion conditions ($I\tau^{1/2}$ constant) to conditions approaching
309 complete depletion ($I\tau$ constant) [44]. These fully depletion conditions are particularly
310 attractive for *in situ* application in samples such as freshwater as they lead to greater
311 sensitivity, and are not affected by adsorption effects [58]. They allow measurements to
312 be made without removing oxygen from the solution [11]. These conditions are
313 therefore suitable for *in situ* analyses of Cu and Pb. The influence of the stripping

314 current on the Cu signal was evaluated in order to establish the experimental conditions
315 under which the complete depletion regime was reached. Figure S5 shows that for the
316 values of I_s between 1 and 20 μA , the complete depletion regime $I\tau$ (constant) is
317 reached from stripping currents between 5 and 20 μA . Regardless of the value of I_s ,
318 plotting $I\tau^{1/2}$ as a function of I_s never resulted in a plateau. As a result, a stripping
319 current of 10 μA was chosen for the following experiments.

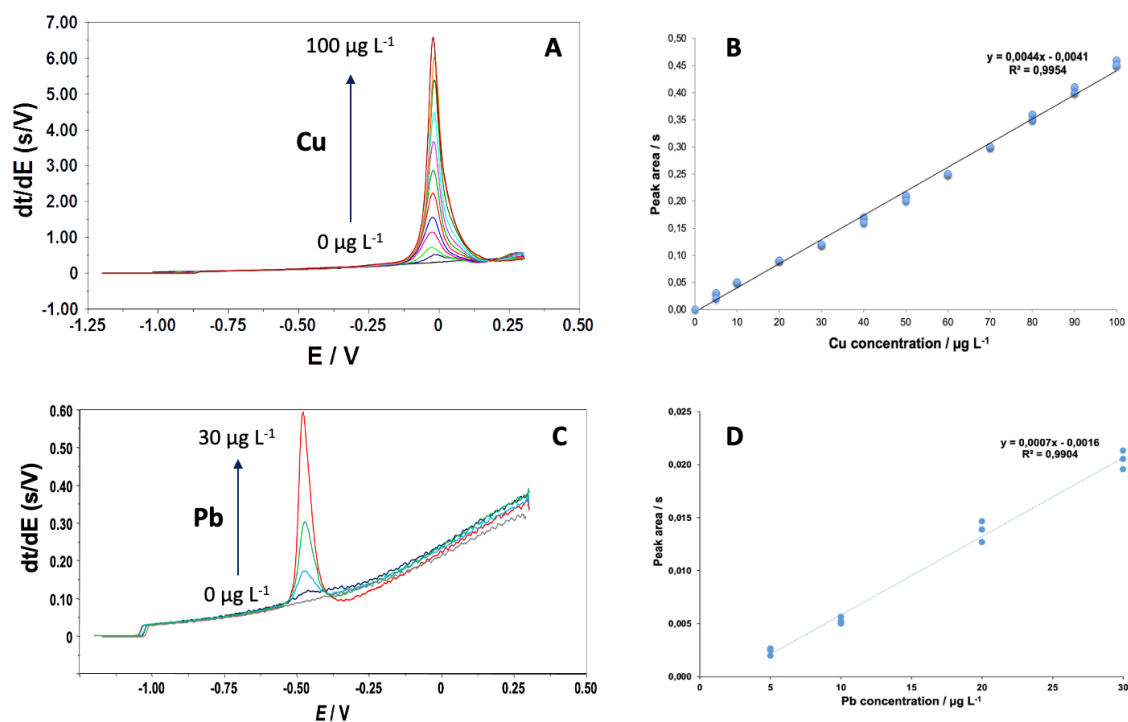
320

321 3.2.2 Analytical performance of the modified SPCE for metals 322 determination

323 The calibration plot for Cu in a sodium acetate solution buffered to pH 4.6 shows that a
324 sensitivity of $0.0044 \pm 0.0005 \text{ s}/\mu\text{g L}^{-1}$ and a linearity of $5 \mu\text{g L}^{-1}$ to $100 \mu\text{g L}^{-1}$ can be
325 obtained, which corresponds to working conditions well suited to the detection of Cu in
326 drinking water (Figure 5A and 6B). A LOD of $2 \mu\text{g L}^{-1}$ and a LOQ of $7 \mu\text{g L}^{-1}$ were
327 obtained for a preconcentration time of 60 s. Similar results were obtained for Pb with a
328 LOD of $2 \mu\text{g L}^{-1}$ and a LOQ of $6 \mu\text{g L}^{-1}$, although this sensor appeared less sensitive for
329 Pb with a slope of $0.00075 \pm 0.00002 \text{ s}/\mu\text{g L}^{-1}$ (Figure 5C and 6D). These results are
330 promising for monitoring purposes as a measurement time of 60 s allows the detection
331 of concentrations in the $\mu\text{g/L}$ range which is in perfect agreement with the values set by
332 legislation.

333 However, these values could be improved by increasing the deposition time since the
334 longer the deposition time, the higher the amount of analyte is available at the electrode
335 during the analysis (Figure S6). Thus, for Pb, increasing the electrodeposition time from
336 60s to 300 s resulted in a calibration line between 100 and 500 ng L^{-1} with a LOD of 63
337 ng L^{-1} and a LOQ of 92 ng L^{-1} (Figure S7). These results are slightly higher than those
338 of Poudel et al for Pb who obtained a LOD of 3.7 ng/L after a waiting time (extraction
339 and reduction) of 1060 s which does not allow continuous *in situ* monitoring [59].
340 Higher concentrations can also be detected by using an electrochemical method less
341 sensitive such as linear scan voltammetry which allows the detection of Cu up to 5 mg
342 L^{-1} (Figure S8). These results show the power of the electrochemistry to detect a wide
343 range of concentrations from ng L^{-1} to mg L^{-1} , only by modifying the electrodeposition
344 time and/or the electrochemical method.

345



346

347 **Figure 5.** Stripping Chronopotentiometric response of Cu (A) and Pb (B) and calibration plot of Cu (C)
 348 and Pb (D) obtained with a modified SPCE in acetate buffer 0.1 mol L⁻¹. Analysis conditions:
 349 electrodeposition: 60 s at -1.2 V with stirring, equilibration time 10 s at -1.2 V without stirring, stripping
 350 current $I_s = 10 \mu\text{A}$ without stirring.

351

352 3.2.3 Repeatability and reproducibility

353 Figure S9 shows Cu signal obtained for 8 modified SPCEs coming from the same
 354 screen-printing plate (Figure S9A) and for 8 modified SPCEs from 8 different screen-
 355 printing plates (Figure S9B). No significant difference was observed between the
 356 different modified electrodes, where a Cu concentration of 20 $\mu\text{g L}^{-1}$ led to a peak area
 357 of $0.064 \text{ s} \pm 0.004 \text{ s}$ for electrodes from the same plate and of $0.072 \text{ s} \pm 0.005 \text{ s}$ for
 358 electrodes from different plates. This result underlines the robustness of the sensor
 359 construction, from serigraphy to modification of the surface, which is promising for the
 360 development of a field sensor.

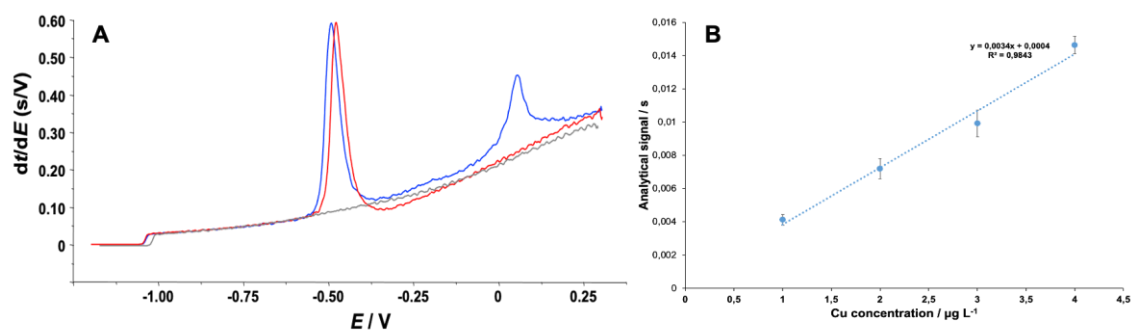
361

362 3.2.4 Simultaneous detection of Cu and Pb

363 Figure 6A shows the Pb signal obtained that simultaneous detection of Pb and Cu is not
 364 a problem as these metals don't have the same redox potential with -0.48 V for Pb and
 365 +0.06 V for Cu. The addition of Cu in the solution doesn't change the Pb signal which
 366 suggests that there is no interference. However, Figure 6B shows that the calibration
 367 plot obtained for Cu concentrations from 1 to 4 $\mu\text{g L}^{-1}$, in the presence of 30 $\mu\text{g L}^{-1}$ of

368 Pb gives a slope of 0.0034 ± 0.0002 s/ $\mu\text{g L}^{-1}$ which is slightly lower than that obtained
369 in the absence of Pb (0.0044 ± 0.0005 s/ $\mu\text{g L}^{-1}$). On the contrary, when the Cu/Pb
370 concentration ratios are reversed, the Cu signal is little affected by the presence of Pb
371 (Figure S10). All these results mean that in the case of a multi-metal contamination, a
372 calibration taking into account the different metals in solution will be necessary to
373 obtain an accurate value.

374



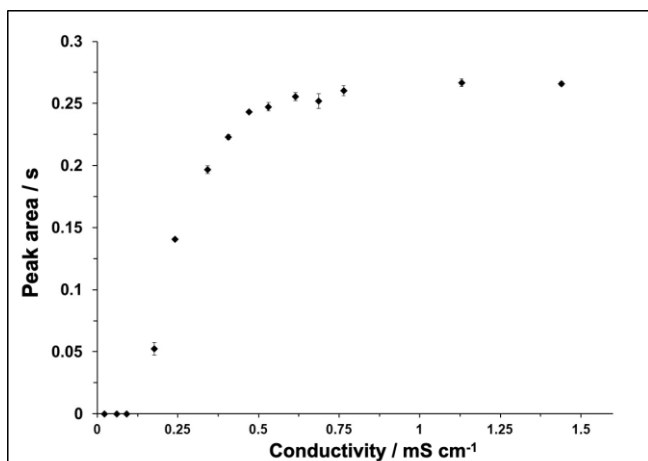
375
376
377
378
379

Figure 6. **A** - Analytical signal of Pb ($30 \mu\text{g L}^{-1}$) without or with Cu ($4 \mu\text{g L}^{-1}$); **B** - Calibration plot of Cu from 1 to 4 $\mu\text{g L}^{-1}$ in presence of Pb at $30 \mu\text{g L}^{-1}$. Analysis conditions: acetate buffer 0.1 mol L^{-1} at pH 4.6, deposition at -1.2 V for 60 s, stripping current $I_s = 10 \mu\text{A}$.

380 3.2.5 Effect of the conductivity of the sample

381 Conductivity is also an important parameter to take into account when analysing natural
382 freshwater samples because this parameter can strongly change from one sample to
383 another. Parat *et al* analysed different natural freshwaters from some rivers in the
384 Pyrenees (France) and found conductivities ranging from 78 to $211 \mu\text{S cm}^{-1}$ [13] while
385 Platikanov *et al* who collected tap waters from different locations in Catalonia (Spain),
386 found conductivities ranging from $82.3 \mu\text{S cm}^{-1}$ to $2417 \mu\text{S cm}^{-1}$ [60]. Therefore, the
387 effects of solution conductivity on Cu signal were studied in ultrapure water doped with
388 Cu at $50 \mu\text{g L}^{-1}$ in which successive additions of acetate (1 mol L^{-1}) were made. Figure
389 7 shows the variation of the signal (peak area) obtained for Cu at different
390 conductivities, with a plateau from a conductivity of $470 \mu\text{S cm}^{-1}$, a value close to those
391 found in most natural freshwaters.

392



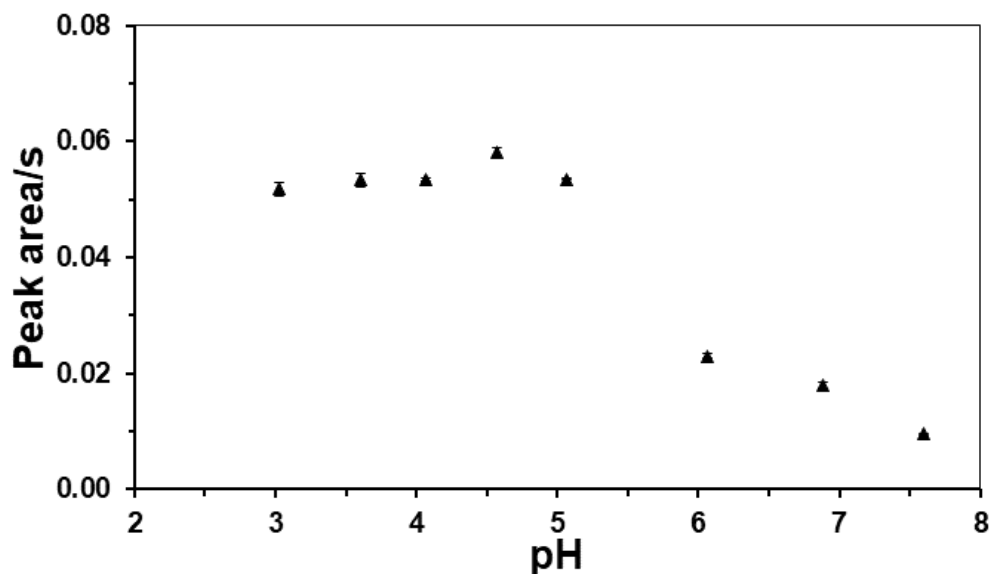
393

394 **Figure 7.** Effect of conductivity on Cu signal (Cu concentration = 50 $\mu\text{g L}^{-1}$) obtained with a modified
 395 SPCE. Analysis conditions: electrodeposition: 60 s at -1.2 V with stirring, equilibration time 10 s at -1.2
 396 V without stirring, stripping current $I_s = 10 \mu\text{A}$ without stirring.

397

398 3.2.6 Effect of pH on water samples

399 The effect of pH on the response of the modified SPCE in the presence of Cu was
 400 studied over a pH range of 3 to 7.6. The pH was adjusted to the different values by
 401 adding acetic acid to mineral water. The signal shows a stable peak area between pH 3
 402 and 5 (Figure 8). At higher pH, a sharp decrease in signal is observed from 57% at pH 6
 403 to 82% at pH 7.6. This behaviour can be due to the inorganic compounds (bicarbonates,
 404 sulphates and nitrates) present in the solution, and capable of forming Cu complexes,
 405 which are not electrolabile. The Visual MINTEQ speciation model confirms that the
 406 proportion of free Cu in mineral water depends on pH with only 3.8 % of free Cu at pH
 407 7.6. At this pH, carbonates appear as the main compound complexing Cu (90%) and
 408 blocking its electrochemical detection (Table 1). Acidification of the sample with acetic
 409 acid from pH 7.6 to 4 changes the Cu speciation leading to 69 % of free Cu and about
 410 27% of Cu-acetate complexes that are electrolabile. Lead shows the same behaviour
 411 with about 88% of Pb-carbonate complexes at pH 7.6 and only 5.6 % of free Pb. The
 412 acidification of the solution leads to a modification of the speciation with about 95% of
 413 labile Pb (Table S1). This means that the determination of the total concentration of Cu
 414 and Pb will require a prior acidification of the solution at pH 5 or less to dissociate Cu
 415 and Pb carbonate complexes present in solution.



416

417 **Figure 8.** Variation of Cu signal according to the pH obtained with a catechol modified SPCE in a
 418 mineral water. Analysis conditions: Cu concentration: $20 \mu\text{g L}^{-1}$, electrodeposition: 60 s at -1.2 V with
 419 stirring, equilibration time 10 s at -1.2 V without stirring, stripping current $I_s = 10 \mu\text{A}$ without stirring.
 420

421 **Table 1.** Speciation of Cu (in %) computed from Visual Minteq 3.0 in mineral water at pH 7.6 and
 422 acidified with acetic acid from pH 7 to 4

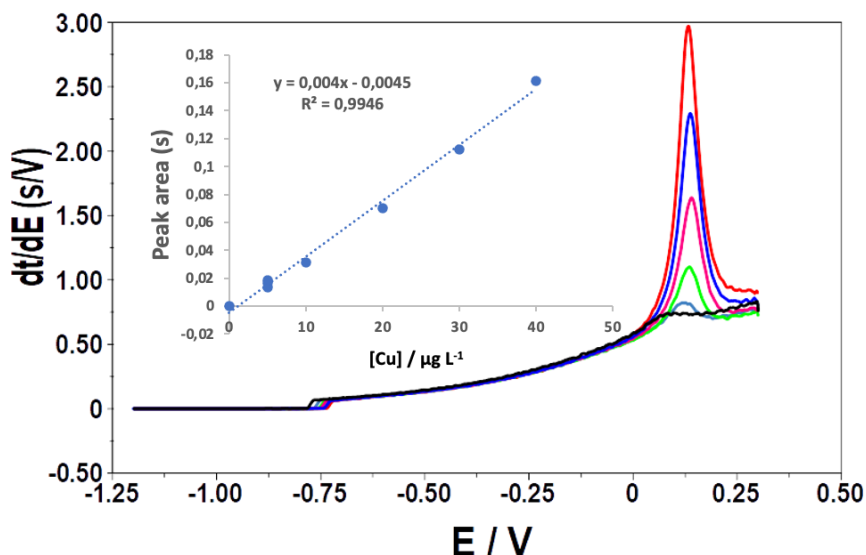
	pH 7.6	pH 7	pH 6	pH 5	pH 4.6	pH 4
Cu^{2+}	3.8	14.9	62.7	69.4	69.1	68.9
CuOH^+	3.7	3.6	1.5	0.2	0.1	
$\text{Cu}(\text{OH})_2$ (aq)	0.2	0.1				
CuCl^+			0.1	0.1	0.1	0.1
CuSO_4 (aq)	0.1	0.6	2.3	2.6	2.6	2.5
CuCO_3 (aq)	89.6	77.7	13.1	0.2		
CuHCO_3^+	0.6	1.9	3.3	0.5	0.2	0.1
Cu-Acetate^+	2.0	0.4	16.5	25.9	26.7	27.2
Cu-(Acetate)_2 (aq)		0.8	0.5	1.1	1.2	1.2

423

424 3.3 Analysis of acidified mineral water by using modified SPCE

425 A calibration plot was carried out in a mineral water sample previously acidified with
 426 acetic acid to dissociate all Cu-complexes (Figure 9) and compared to that obtained in
 427 acetate solution. The deposition time and SCP parameters were the same as those used
 428 previously. A slope of $0.0041 \text{ s}/\mu\text{g L}^{-1}$ was obtained in acidified mineral water which is
 429 similar to that obtained in 0.1 mol L^{-1} acetate buffer ($0.0044 \pm 0.0005 \text{ s}/\mu\text{g L}^{-1}$) showing
 430 that no interfering effect occurs in a solution such as a mineral water.

431



432 **Figure 9.** Stripping chronopotentiometric response and Cu calibration plot obtained with modified SPE
 433 sensor in the presence of different copper concentrations in acidified mineral water (pH 4). Analysis
 434 conditions: electrodeposition: 60 s at -1.2 V with stirring, equilibration time 10 s at -1.2 V without
 435 stirring, stripping current $I_s = 10 \mu\text{A}$ without stirring.
 436
 437

438 **4. Conclusion**

439 A new electrochemical sensor has been developed for the detection of Cu and Pb in
 440 acidified drinking water. For this purpose, a screen-printed carbon electrode was
 441 modified by a polycatechol film. Different parameters were studied to obtain a
 442 homogeneous and stable film, as the effect of pH, the scan rate and the number of
 443 electropolymerisation scans. Optimisation of the polymerisation conditions resulted in a
 444 highly reproducible electrochemical platform indicating a simple and robust method of
 445 sensor fabrication.

446 High performance was achieved using stripping chronopotentiometry (SCP) to detect Cu
 447 and Pb in acetate buffer at pH 4.6. We showed the power of the electrochemistry to
 448 detect a wide range of concentrations from ng L^{-1} to mg L^{-1} with the same working
 449 electrode, only by modifying the electrodeposition time and/or the electrochemical
 450 method (SCP or LSV).

451 From a more general point of view, compared to previous studies aimed at developing
 452 electrochemical sensors for trace metal detection in drinking water, we demonstrate for
 453 the first time an efficient and sensitive electrode based on a polycatechol film. This
 454 preparation method is interesting because it can easily replace the deposition of
 455 expensive, toxic (mercury film) and sometimes complicated synthetic molecules like
 456 cyclodextrins and calixarene used for detection of trace metal such as Cu. The analytical
 457 performances obtained, namely a good reproducibility, a good repeatability and a

458 sensitivity range in agreement with the concentrations found in acidified mineral water
459 for Pb and Cu for measurement time between 60 s and 300s, make this modified SPCE
460 an ideal candidate for industrialisation for monitoring the aquatic environment.
461 Research is underway to develop an industrial sensor where the three electrodes
462 (working, auxiliary and reference) would be combined on a single sensor.

463

464 **Acknowledgments**

465 We would like to acknowledge the financial support of our collaborator “SYCLOPE
466 ELECTRONIQUE” for the industrial project “GREEN SENSOR”.

467

468 **References**

- 469 [1] L. Chang, J.H.W. Lee, Y.S. Fung, Prediction of lead leaching from galvanic
470 corrosion of lead-containing components in copper pipe drinking water supply systems,
471 *J Hazard Mater* 436 (2022) 129169.
- 472 [2] WHO, Guidelines for drinking-water quality: fourth edition incorporating the first
473 and second addenda., World Health Organization (WHO), Geneva, 2022, p. 614.
- 474 [3] WHO, Copper in Drinking-water, Guidelines for Drinking-water Quality, World
475 Health Organization (WHO), 2004, p. 31.
- 476 [4] Directive 2020/2184/EU of the european parliament and of the council of 16
477 December 2020 on the quality of water intended for human consumption, Official
478 Journal of the European Union, 2020, p. 62.
- 479 [5] WHO, Lead in drinking-water: Health risks, monitoring and corrective actions,
480 World Health Organization (WHO), 2022, p. 26.
- 481 [6] P.M. Madhu, R.S. Sadagopan, Effect of Heavy Metals on Growth and Development
482 of Cultivated Plants with Reference to Cadmium, Chromium and Lead – A Review,
483 *Journal of Stress Physiology & Biochemistry* 16 (2020) 84-102.
- 484 [7] S. Hussain, T. Sultana, S. Sultana, B. Hussain, S. Mahboob, K.A. Al-Ghanim, M.N.
485 Riaz, Seasonal monitoring of River through heavy metal bioaccumulation and
486 histopathological alterations in selected fish organs, *Journal of King Saud University -*
487 *Science* 33(8) (2021).
- 488 [8] M. Cuartero, Electrochemical sensors for in-situ measurement of ions in seawater,
489 *Sensors and Actuators B: Chemical* 334 (2021) 129635.
- 490 [9] S. Betelu, C. Parat, N. Petrucciani, A. Castetbon, L. Authier, M. Potin-Gautier,
491 Semicontinuous monitoring of cadmium and lead with a screen-printed sensor modified
492 by a membrane, *Electroanalysis* 19(2-3) (2007) 399-402.
- 493 [10] C. Parat, L. Authier, S. Betelu, N. Petrucciani, M. Potin-Gautier, Determination of
494 labile cadmium using a screen-printed electrode modified by a microwell,
495 *Electroanalysis* 19 (2007) 403-406.
- 496 [11] C. Parat, A. Schneider, A. Castetbon, M. Potin-Gautier, Determination of trace
497 metal speciation parameters by using screen-printed electrodes in stripping
498 chronopotentiometry without deaerating, *Analytica Chimica Acta* 688 (2011) 156-162.
- 499 [12] O. Zaouak, L. Authier, C. Cugnet, A. Castetbon, M. Potin-Gautier,
500 Electroanalytical device for cadmium speciation in waters. Part 1: Development and

501 characterization of a reliable screen-printed sensor, *Electroanalysis* 22 (2010) 1151-
502 1158.

503 [13] C. Parat, L. Authier, A. Castetbon, D. Aguilar, E. Companys, J. Puy, J. Galceran,
504 M. Potin-Gautier, Free Zn²⁺ determination in natural freshwater of the Pyrenees:
505 towards on-site measurements with AGNES, *Environmental Chemistry* 12 (2015) 329-
506 337.

507 [14] H. Xiang, Q. Cai, Y. Li, Z. Zhang, L. Cao, K. Li, H. Yang, Sensors Applied for the
508 Detection of Pesticides and Heavy Metals in Freshwaters, *Journal of Sensors* 2020
509 (2020) 1-22.

510 [15] O.D. Renedo, M. Julia Arcos Martinez, A novel method for the anodic stripping
511 voltammetry determination of Sb(III) using silver nanoparticle-modified screen-printed
512 electrodes, *Electrochemistry Communications* 9(4) (2007) 820-826.

513 [16] M. Li, Y.-T. Li, D.-W. Li, Y.-T. Long, Recent developments and applications of
514 screen-printed electrodes in environmental assays - A review, *Analytica Chimica Acta*
515 734(0) (2012) 31-44.

516 [17] X. Liu, Y. Yao, Y. Ying, J. Ping, Recent advances in nanomaterial-enabled screen-
517 printed electrochemical sensors for heavy metal detection, *TrAC Trends in Analytical*
518 *Chemistry* 115 (2019) 187-202.

519 [18] A. García-Miranda Ferrari, P. Carrington, S.J. Rowley-Neale, C.E. Banks, Recent
520 advances in portable heavy metal electrochemical sensing platforms, *Environmental*
521 *Science: Water Research & Technology* 6(10) (2020) 2676-2690.

522 [19] J.-Y. Choi, K. Seo, S.-R. Cho, J.-R. Oh, S.-H. Kahng, J. Park, Screen-printed
523 anodic stripping voltammetric sensor containing HgO for heavy metal analysis,
524 *Analytica Chimica Acta* 443(2) (2001) 241-247.

525 [20] K.C. Honeychurch, J.P. Hart, Screen-printed electrochemical sensors for
526 monitoring metal pollutants, *TrAC Trends in Analytical Chemistry* 22(7) (2003) 456-
527 469.

528 [21] C. Parat, S. Betelu, L. Authier, M. Potin-Gautier, Determination of labile trace
529 metals with screen-printed electrode modified by a crown-ether based membrane,
530 *Analytica Chimica Acta* 573-574 (2006) 14-19.

531 [22] W. Wang, Stripping Analysis at Bismuth Electrodes: A Review, *Electroanalysis*
532 17(15-16) (2005) 1341-1346.

533 [23] I. Svancara, L. Baldrianová, E. Tesarová, S.B. Hocevar, A.A. Elsuccary, A.
534 Economou, S. Sotiropoulos, B. Ogorevc, K. Vytras, Recent Advances in Anodic
535 Stripping Voltammetry with Bismuth-Modified Carbon Paste Electrodes,
536 *Electroanalysis* 18(2) (2006) 177-185.

537 [24] A. Sanchez-Calvo, M.C. Blanco-Lopez, A. Costa-Garcia, Paper-Based Working
538 Electrodes Coated with Mercury or Bismuth Films for Heavy Metals Determination,
539 *Biosensors (Basel)* 10 (2020) bios10050052.

540 [25] S. Laschi, I. Palchetti, M. Mascini, Gold-based screen-printed sensor for detection
541 of trace lead, *Sensors and Actuators B: Chemical* 114(1) (2006) 460-465.

542 [26] P. Salaün, B. Planer-Friedrich, C.M.G. van den Berg, Inorganic arsenic speciation
543 in water and seawater by anodic stripping voltammetry with a gold microelectrode,
544 *Analytica Chimica Acta* 585(2) (2007) 312-322.

545 [27] R.D. Riso, M. Waeles, P. Monbet, C.J. Chaumery, Measurements of trace
546 concentrations of mercury in sea water by stripping chronopotentiometry with gold disk
547 electrode: influence of copper, *Analytica Chimica Acta* 410(1-2) (2000) 97-105.

548 [28] Z. Ait-Touchente, S. Falah, E. Scavetta, M.M. Chehimi, R. Touzani, D. Tonelli, A.
549 Taleb, Different Electrochemical Sensor Designs Based on Diazonium Salts and Gold
550 Nanoparticles for Pico Molar Detection of Metals, *Molecules* 25(17) (2020).

- 551 [29] M.B. Gumpu, S. Sethuraman, U.M. Krishnan, J.B.B. Rayappan, A review on
552 detection of heavy metal ions in water – An electrochemical approach, *Sensors and*
553 *Actuators B: Chemical* 213(0) (2015) 515-533.
- 554 [30] L. Cui, J. Wu, H. Ju, Electrochemical sensing of heavy metal ions with inorganic,
555 organic and bio-materials, *Biosensors and Bioelectronics* 63(0) (2015) 276-286.
- 556 [31] O. Kanoun, T. Lazarevic-Pasti, I. Pasti, S. Nasraoui, M. Talbi, A. Brahem, A.
557 Adiraju, E. Sheremet, R.D. Rodriguez, M. Ben Ali, A. Al-Hamry, A Review of
558 Nanocomposite-Modified Electrochemical Sensors for Water Quality Monitoring,
559 *Sensors (Basel)* 21(12) (2021) s21124131.
- 560 [32] D. Tyagi, H. Wang, W. Huang, L. Hu, Y. Tang, Z. Guo, Z. Ouyang, H. Zhang,
561 Recent advances in two-dimensional-material-based sensing technology toward health
562 and environmental monitoring applications, *Nanoscale* 12(6) (2020) 3535-3559.
- 563 [33] C. Kumunda, A.S. Adekunle, B.B. Mamba, N.W. Hlongwa, T.T.I. Nkambule,
564 Electrochemical Detection of Environmental Pollutants Based on Graphene Derivatives:
565 A Review, *Frontiers in Materials* 7 (2021) 616787.
- 566 [34] A.M. Sanjuán, J.A. Reglero Ruiz, F.C. García, J.M. García, Recent developments
567 in sensing devices based on polymeric systems, *React Funct Polym* 133 (2018) 103-
568 125.
- 569 [35] X. Zheng, S. Khaoulani, N. Ktari, M. Lo, A.M. Khalil, C. Zerrouki, N. Fourati,
570 M.M. Chehimi, Towards Clean and Safe Water: A Review on the Emerging Role of
571 Imprinted Polymer-Based Electrochemical Sensors, *Sensors (Basel)* 21(13) (2021).
- 572 [36] Y. Wang, A. Liu, Y. Han, T. Li, Sensors based on conductive polymers and their
573 composites: a review, *Polymer International* 69 (2020) 7-17.
- 574 [37] E. Faure, C. Falentin-Daudré, C. Jérôme, J. Lyskawa, D. Fournier, P. Woisel, C.
575 Detrembleur, Catechols as versatile platforms in polymer chemistry, *Progress in*
576 *Polymer Science* 38(1) (2013) 236-270.
- 577 [38] L.C. Almeida, R.D. Correia, B. Palys, J.P. Correia, A.S. Viana, Comprehensive
578 Study of the Electrochemical Growth and Physicochemical Properties of
579 Polycatecholamines and Polycatechol, *Electrochimica Acta* (2021).
- 580 [39] V.T. Athavale, L.H. Prabhu, D.G. Vartak, Solution stability constants of some
581 metal complexes of derivatives of catechol, *Journal of Inorganic and Nuclear Chemistry*
582 28(5) (1966) 1237-1249.
- 583 [40] A.E. Martell, R.M. Smith, Critical stability constants: Other Organic Ligands,
584 1977.
- 585 [41] V.M. Vorotyntsev, E.P. Kuznetsova, Y.I. Pyatnitskii, G.I. Golodets, Homogeneous
586 catalytic oxidation of pyrocatechol in the presence of transition metal ions, *React Kinet*
587 *Catal Lett* 13(4) (1980) 373-378.
- 588 [42] A. Bačinić, L.-M. Tumir, M. Mlakar, Electrochemical characterization of
589 Cobalt(II)-Complexes involved in marine biogeochemical processes. I. Co(II)-4-
590 nitrocatechol and Co(II)-Humate, *Electrochimica Acta* 337 (2020) 135797.
- 591 [43] S.B. Khoo, J. Zhu, Poly(catechol) Film Modified Glassy Carbon Electrode for
592 Ultratrace Determination of Cerium(III) by Differential Pulse Anodic Stripping
593 Voltammetry, *Electroanalysis* 11(8) (1999) 546-552.
- 594 [44] R.M. Town, H.P. van Leeuwen, Fundamental features of metal ion determination
595 by stripping chronopotentiometry, *Journal of Electroanalytical Chemistry* 509(1) (2001)
596 58-65.
- 597 [45] H.P. van Leeuwen, R.M. Town, Elementary features of depletive stripping
598 chronopotentiometry, *Journal of Electroanalytical Chemistry* 535(1-2) (2002) 1-9.

- 599 [46] A. Shrivastava, V. Gupta, Methods for the determination of limit of detection and
600 limit of quantitation of the analytical methods, *Chronicles of Young Scientists* 2(1)
601 (2011).
- 602 [47] J.P. Gustafsson, Visual Minteq, version 3.0,
603 <http://www2.lwr.kth.se/English/OurSoftware/vminteq/> (2010).
- 604 [48] M.D. Ryan, A. Yueh, W.-Y. Chen, The Electrochemical Oxidation of Substituted
605 Catechols, *Journal of The Electrochemical Society* 127 (1980) 1489-1495.
- 606 [49] T. Palomäki, S. Chumillas, S. Sainio, V. Protopopova, M. Kauppila, J. Koskinen,
607 V. Climent, J.M. Feliu, T. Laurila, Electrochemical reactions of catechol,
608 methylcatechol and dopamine at tetrahedral amorphous carbon (ta-C) thin film
609 electrodes, *Diamond and Related Materials* 59 (2015) 30-39.
- 610 [50] J. Bai, X. Bo, B. Qi, L. Guo, A Novel Polycatechol/Ordered Mesoporous Carbon
611 Composite Film Modified Electrode and Its Electrocatalytic Application,
612 *Electroanalysis* 22(15) (2010) 1750-1756.
- 613 [51] B. Marczewska, M. Przegaliński, Poly(catechol) electroactive film and its
614 electrochemical properties, *Synthetic Metals* 182(0) (2013) 33-39.
- 615 [52] A. Raouafi, A. Rabti, N. Raouafi, A printed SWCNT electrode modified with
616 polycatechol and lysozyme for capacitive detection of α -lactalbumin, *Microchimica*
617 *Acta* 184 (2017) 4351-4357.
- 618 [53] S. Kim, C. Silva, D.V. Evtuguin, J.A. Gamelas, A. Cavaco-Paulo,
619 Polyoxometalate/laccase-mediated oxidative polymerization of catechol for textile
620 dyeing, *Appl Microbiol Biotechnol* 89(4) (2011) 981-7.
- 621 [54] V. Ball, Electrodeposition of pyrocatechol based films: Influence of potential scan
622 rate, pyrocatechol concentration and pH, *Colloids and Surfaces A: Physicochemical and*
623 *Engineering Aspects* 518 (2017) 109-115.
- 624 [55] R. Romero, P.R. Salgado, C. Soto, D. Contreras, V. Melin, An Experimental
625 Validated Computational Method for pKa Determination of Substituted 1,2-
626 Dihydroxybenzenes, *Front Chem* 6 (2018) 208.
- 627 [56] R. Pourghobadi, D. Nematollahi, M.R. Baezzat, S. Alizadeh, H. Goljani,
628 Electropolymerization of catechol on wireless graphite electrode. Unusual cathodic
629 polycatechol formation, *Journal of Electroanalytical Chemistry* 866 (2020) 114180.
- 630 [57] L.C. Almeida, R.D. Correia, A. Marta, G. Squillaci, A. Morana, F. La Cara, J.P.
631 Correia, A.S. Viana, Electrosynthesis of polydopamine films - tailored matrices for
632 laccase-based biosensors, *Applied Surface Science* 480 (2019) 979-989.
- 633 [58] R.M. Town, H.P. van Leeuwen, Effects of adsorption in stripping
634 chronopotentiometric metal speciation analysis, *Journal of Electroanalytical Chemistry*
635 523(1-2) (2002) 1-15.
- 636 [59] A. Poudel, G.S. Shyam Sunder, A. Rohanifar, S. Adhikari, J.R. Kirchoff,
637 Electrochemical determination of Pb²⁺ and Cd²⁺ with a poly(pyrrole-1-carboxylic
638 acid) modified electrode, *Journal of Electroanalytical Chemistry* 911 (2022).
- 639 [60] S. Platikanov, D. Baquero, S. Gonzalez, J. Martin-Alonso, M. Paraira, J.L. Cortina,
640 R. Tauler, Chemometric analysis for river water quality assessment at the intake of
641 drinking water treatment plants, *Sci Total Environ* 667 (2019) 552-562.

642